Tunable Rashba Spin-Orbit Interaction at Oxide Interfaces

A. D. Caviglia,[1] M. Gabay,[2] S. Gariglio,[1] N. Reyren,[1] C. Cancellieri,[1] and J.-M. Triscone[1]

[1]*Département de Physique de la Matière Condensée, University of Geneva, 24 Quai Ernest-Ansermet, 1211 Genève 4, Switzerland*
[2]*Laboratoire de Physique des Solides, Batiment 510, Université Paris-Sud 11, Centre d'Orsay, 91405 Orsay Cedex, France*

(Received 11 January 2010; published 26 March 2010)

The quasi-two-dimensional electron gas found at the $LaAlO_3/SrTiO_3$ interface offers exciting new functionalities, such as tunable superconductivity, and has been proposed as a new nanoelectronics fabrication platform. Here we lay out a new example of an electronic property arising from the interfacial breaking of inversion symmetry, namely, a large Rashba spin-orbit interaction, whose magnitude can be modulated by the application of an external electric field. By means of magnetotransport experiments we explore the evolution of the spin-orbit coupling across the phase diagram of the system. We uncover a steep rise in Rashba interaction occurring around the doping level where a quantum critical point separates the insulating and superconducting ground states of the system.

DOI: 10.1103/PhysRevLett.104.126803 PACS numbers: 71.70.Ej, 73.20.−r, 73.43.Nq, 74.25.Dw

One of the major quests of modern electronics is the search for new functionalities in solid state nanoscale devices. In that respect, high hopes have been placed on spintronics, where information is processed by manipulating the electrons spin in addition to their charge [1]. The spin field effect transistor is certainly the paradigm of this new approach [2]. In this device the Rashba spin-orbit coupling [3] is used to control the spin precession in a two-dimensional electron gas confined in conventional semiconductors heterostructures [4–6]. Another interesting and potentially rewarding strategy is to develop spintronic devices based on interfaces between complex oxides, where new and unusual electronic phases are promoted [7–10]. In these systems, the Rashba interaction, arising from the breaking of structural inversion symmetry, can be substantial and play a critical role in controlling interfacial electronic states absent in the constituent materials. It has recently been shown that the ground state of the metallic interface between the band insulators $LaAlO_3$ and $SrTiO_3$ can be driven through a quantum phase transition from an insulating to a superconducting state [11]. In this Letter we show that a strong Rashba spin-orbit interaction is present in this system and that its magnitude can be tuned with an external electric field. Remarkably, a steep rise of the Rashba coupling occurs across the quantum critical point separating the insulating and superconducting ground states of the system.

It has been recently demonstrated by transport experiments [12] and conductive atomic force microscopy [13,14] that the electron gas present in $LaAlO_3/SrTiO_3$ heterostructures grown using appropriate conditions is confined within a few nanometers from the interface. This structural configuration breaks inversion symmetry and, as a result, the electron gas confined in the vicinity of a polar interface [7] will experience a strong electric field directed perpendicular to the conduction plane. To provide an accurate representation of this internal electric field, the large local polarization of $SrTiO_3$ caused by its massive, electric field dependent, low temperature permittivity ($\epsilon_r > 10^4$) has to be considered [14]. A new class of physical phenomena occurring because of the presence of this effective electric field are captured by the Rashba Hamiltonian [3] $H_R = \alpha(\hat{n} \times \vec{k}) \cdot \vec{S}$, where $\vec{S}$ are the Pauli matrices, $\vec{k}$ is the electron wave vector and $\hat{n}$ is a unit vector perpendicular to the interface. This Hamiltonian describes the coupling of the electrons spin to an internal magnetic field $\propto \hat{n} \times \vec{k}$, experienced in their rest frame, which is perpendicular to their wave vector and lies in the plane of the interface. One important consequence of this interaction is that the dispersion relation of the electrons divides into two branches separated at the Fermi surface by a spin splitting $\Delta = 2\alpha k_F$, k_F being the Fermi wave vector and α the strength of the spin-orbit coupling. Perhaps the most appealing feature of this interaction is that its coupling constant is related to the electric field experienced by the electrons and can be therefore tuned by applying an external gate voltage [5,6]. Aiming to explore this phenomenon in $LaAlO_3/SrTiO_3$ interfaces, we fabricated field effect devices as discussed in Ref. [11]. In our field effect experiments the modulation of the total electric field experienced by the electron gas is particularly effective thanks to the special dielectric properties of $SrTiO_3$.

The magnetic field dependence of the conductance underscores the intriguing coupling between spin dynamics and transport. Figure 1(a) shows the magnetoconductance $[\sigma(H) - \sigma(H = 0)]/\sigma(H = 0)$ (σ being the sheet conductance and H the applied magnetic field), measured in a magnetic field applied perpendicular to the $LaAlO_3/SrTiO_3$ interface at a temperature $T = 1.5$ K for gate voltages V between -300 V and $+200$ V. Measurements performed in a parallel field configuration are presented and discussed in Ref. [15]. The magnetoconductance measurements are carried out using a standard

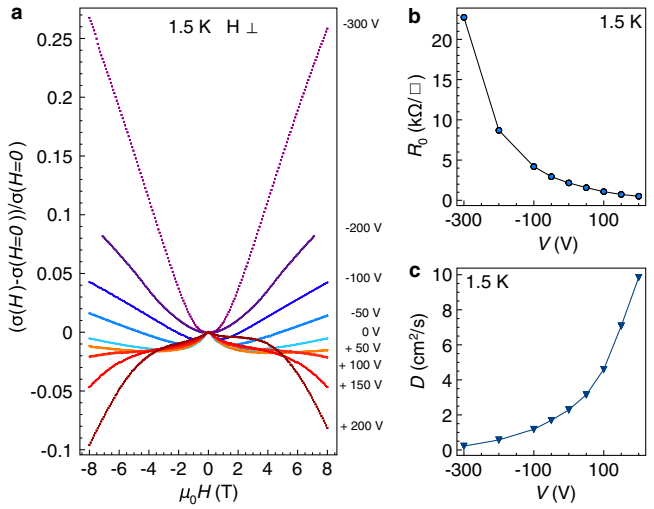

FIG. 1 (color online). Modulation of the transport properties of the $LaAlO_3/SrTiO_3$ interface under electric and magnetic fields. (a) Magnetoconductance $[\sigma(H) - \sigma(H = 0)]/\sigma(H = 0)$ (σ being the sheet conductance, and H the applied magnetic field) measured at 1.5 K in perpendicular magnetic field for different applied gate voltages. (b) Sheet resistance (R_0) modulation resulting from the field effect measured at 1.5 K. (c) Field effect modulation of the diffusion coefficient D estimated at 1.5 K.

four points dc technique. As shown in Fig. 1(a), for large negative gate voltages we observe a large positive magnetoconductance that exceeds +25% at 8 T and −300 V. As we increase the voltage ($V > -200$ V), a low field regime characterized by a negative magnetoconductance appears. Increasing the gate voltage further, we observe that the negative magnetoconductance regime widens out. For the largest applied electric field, we observe that the magnetoconductance remains negative up to the largest accessible magnetic field (8 T). This behavior has been observed in several samples. Similar modulations of magnetoconductance have already been observed in metallic thin films [16] and semiconductor heterostructures [5,6]. Here, the large electrostatic tunability of the magnetoconductance observed in $LaAlO_3/SrTiO_3$ heterostructures is an explicit example of a transport phenomenon occurring at an oxide interface, never observed in its constituent materials. A possible interpretation of this phenomenon is based on the presence of a strong spin-orbit interaction which counteracts weak localization (weak antilocalization) [17]. The spin-orbit relaxation time is an essential ingredient to describe transport in a two-dimensional electron gas in the presence of a strong homogeneous electric field. As previously discussed, the conduction electrons will experience an internal magnetic field which is always perpendicular to their wave vector $\vec{k}$. In a diffusive system this vector will rotate at every scattering event causing rapid fluctuations of the internal magnetic field. These fluctuations will affect the evolution of the spin phase and will define a spin relaxation time τ_{so}. This is known as the D'yakonov-Perel' (DP) mechanism of spin relaxation [18]. In this scenario, the Rashba coupling constant α and the spin relaxation time τ_{so} are related through $\tau_{so} = \hbar^4/4\alpha^2 m^2 2D$, where m is the carrier mass and D the diffusion constant. A second class of spin relaxation processes, known as the Elliott-Yafet (EY) mechanism, originates from the spin-orbit interaction of the lattice ions with the conduction electrons [19,20]. This spin relaxation mechanism can become relevant in the presence of strong spin-orbit scattering impurities or whenever the ionic spin-orbit coupling produces a significant correction to the band structure of the material. In the case of $SrTiO_3$, band structure calculations show that the Ti $3d$ conduction bands are notably altered by this correction [21]. Therefore, in principle both mechanisms can be at play at the $LaAlO_3/SrTiO_3$ interfaces. Nevertheless, one can identify the dominant mechanism by studying the dependence of the spin relaxation time on the elastic scattering time τ [1]. In the case of the EY mechanism (ionic spin-orbit interaction), the Elliott relation $\tau_{so} \sim \tau/(\Delta g)^2$ (Δg is the difference between the electrons g factor in the solid and the one of free electrons) predicts a direct proportionality between the spin relaxation time and the elastic scattering time. In a DP scenario (Rashba spin-orbit interaction) the spin relaxation time should be inversely proportional to the elastic scattering time $\tau_{so} \sim 1/\tau$.

The influence of the spin-orbit interaction can be assessed by measuring the magnetoconductivity in the diffusive regime. In a two-dimensional layer with in-plane spin-orbit relaxation time, immersed in a perpendicular magnetic field H, and in the limit $H < H_{so} = \hbar/4eD\tau_{so}$, the first order correction to the conductance $\Delta\sigma$ takes the Maekawa-Fukuyama (MF) form [15,22])

$$\frac{\Delta\sigma(H)}{\sigma_0} = \Psi\left(\frac{H}{H_i + H_{so}}\right) + \frac{1}{2\sqrt{1-\gamma^2}}\Psi\left(\frac{H}{H_i + H_{so}(1+\sqrt{1-\gamma^2})}\right) - \frac{1}{2\sqrt{1-\gamma^2}}\Psi\left(\frac{H}{H_i + H_{so}(1-\sqrt{1-\gamma^2})}\right).$$

The function Ψ is defined as $\Psi(x) = \ln(x) + \psi(\frac{1}{2} + \frac{1}{x})$, where $\psi(x)$ is the digamma function and $\sigma_0 = e^2/\pi h$ is a universal value of conductance. The parameters of the theory are the inelastic field $H_i = \hbar/4eD\tau_i$, H_{so} and the electrons g factor g which enters into the Zeeman correction $\gamma = g\mu_B H/4eDH_{so}$. μ_B is the Bohr magneton and τ_i is the inelastic scattering time. Since we perform our experiments at 1.5 K, which is at least 5 times the maximum superconducting critical temperature, we can neglect superconducting fluctuations. In a magnetotransport experiment we can then quantify the two relevant time scales of the problem, namely τ_{so} and τ_i. The MF theory has been used to fit the experimental data of Fig. 1(a) in terms of variation of conductance with respect to $e^2/\pi h \simeq 1.2 \times 10^{-5}$ S. Since the effective mass (the elastic scattering time) is 1 to 2 orders of magnitude larger (smaller) than

the corresponding quantities for typical semiconductors, the diffusive regime holds for fields up to 4 T. As the MF theory is based on a perturbative expansion, we have also checked that the magnetoresistance and magnetoconductance are still equal in absolute value up to 4 T. For the range of fields and gate voltages (up to 100 V [23]) that we analyzed, weak localization corrections dominate Coulomb interaction contributions. The best fits are presented in Fig. 2(a), where we observe a remarkable agreement between theory and experiments. This analysis allows us to trace the electric field dependence of the parameters $H_{i,\mathrm{so}}$, presented in Fig. 2(b), and γ. Analyses of the magnetoconductance performed using expressions derived by Punnoose [24] provide the same evolution of the characteristic fields. To extract from these parameters the relaxation times $\tau_{i,\mathrm{so}}$ and the electrons g factor, we need to determine the electric field dependence of the diffusion coefficient. For this purpose we measured the electric field modulation of the sheet carrier concentration $n_{2\mathrm{D}}$ by means of Hall effect and by capacitance measurements [11]. An estimate of the Fermi velocity v_F and of the elastic scattering time using a parabolic dispersion relation with an effective mass $m^* = 3m_e$ [21] (m_e is the bare electron mass), and data collected at the temperature $T = 1.5$ K, allows the diffusion coefficient to be derived as $D = v_F^2\tau/2$. D as a function of V is plotted in Fig. 1(c).

The gate voltage dependence of the g factor is presented in Fig. 2(c). One observes a large increase from a small value, around 0.5 for negative voltages, towards the typical value of 2 for bare electrons at positive voltages. An electric field control of the g factor has been previously predicted [25] and experimentally demonstrated [26] in semiconductor heterostructures. We now turn to the issue of the gate voltage dependence of the parameters $H_{i,\mathrm{so}}$ that will allow us to discern the modulation of spin-orbit coupling brought about by the electric field. The relaxation times $\tau_{i,\mathrm{so}}$ are plotted against gate voltage in Fig. 3(a). For large negative gate voltages we observe that the inelastic scattering time is shorter than the spin relaxation time, indicating that the effect of the spin-orbit interaction is weak compared with the orbital effect of the magnetic field. In this regime, the quantum correction to the conductivity can be ascribed to weak localization, in agreement with the observed temperature evolution of the conductivity [11]. Above a critical voltage the spin relaxation time becomes shorter than the inelastic scattering time and decreases sharply, by 3 orders of magnitude, as the voltage is increased. By contrast, the inelastic scattering time remains fairly constant as we increase the voltage. Here a weak antilocalization regime appears, characterized by a strong spin-orbit interaction. As previously discussed, the nature of the spin-orbit mechanism can be discerned by examining the dependence of the spin relaxation time on the elastic scattering time. In Fig. 3(a) we show the gate voltage dependence of the spin relaxation time predicted by the Elliott relation, calculated using the electrons g factor presented in Fig. 2(c). Clearly, the EY mechanism fails to estimate the spin relaxation time by 3 orders of magnitude at -300 V and its predicted variation with V is opposite to that observed. In fact, as can be seen in

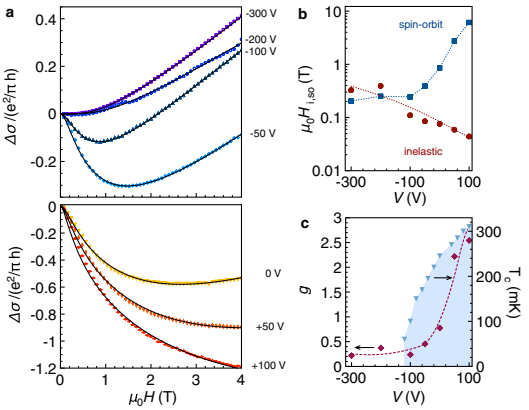

FIG. 2 (color online). Analysis of the magnetoconductivity of the $LaAlO_3/SrTiO_3$ interface. (a) Best fits according to the Maekawa-Fukuyama theory of the variation of conductance $\Delta\sigma$, normalized with respect to $e^2/\pi h$, for different gate voltages. (b) Gate voltage dependence of the fitting parameters H_i (red dots) and H_{so} (blue squares). The lines are a guide to the eye. (c) Left axis, purple diamonds: gate voltage dependence of the electrons g factor g. The line is a guide to the eye. Right axis, blue triangles: superconducting critical temperature T_c as a function of gate voltage for the same sample.

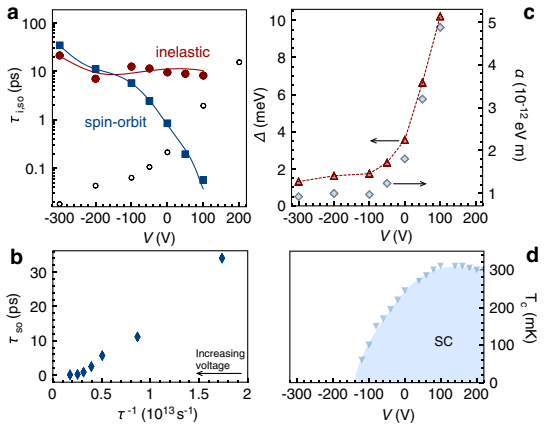

FIG. 3 (color online). Rashba control of the $LaAlO_3/SrTiO_3$ interface electronic phase diagram. (a) Inelastic relaxation time τ_i (red circles) and spin relaxation time τ_{so} (blue squares) as a function of gate voltage plotted on a logarithmic time scale. The lines are a guide to the eye. Prediction of the spin relaxation time as a function of gate voltage based on the Elliott relation (open circles). (b) Spin relaxation time vs elastic scattering rate showing consistency with the D'yakonov-Perel' mechanism. (c) Left axis, red triangles: field effect modulation of the Rashba spin splitting Δ. Right axis, gray diamonds: field effect modulation of the Rashba coupling constant α. (d) Superconducting critical temperature T_c as a function of gate voltage for the same sample. Note that the crossing of the inelastic and spin relaxation times occurs at the quantum critical point.

Fig. 3(b), the spin relaxation time is proportional to the inverse of the elastic scattering time over a wide voltage range, a clear signature of the DP mechanism characteristic of the Rashba spin-orbit interaction. For $V > 50$ V, a deviation from the DP relation is experimentally observed. This deviation coincides with the departure from the collision-dominated regime which occurs as τ_{so} becomes of order τ. This evolution points towards a strong spin-orbit coupling where an electron spin may precess through several cycles before scattering. These observations indicate that the unusually strong and tunable spin-orbit interaction found in $LaAlO_3/SrTiO_3$ heterostructures arises from the interfacial breaking of inversion symmetry.

A remarkable correlation between the onset of strong spin fluctuations and the emergence of superconductivity is evident by comparing Figs. 3(a) and 3(d), where we notice that the superconducting dome, measured on the same sample, develops as the spin relaxation time becomes significantly smaller than the inelastic scattering time. This finding suggests that the spin-orbit interaction plays an important role in stabilizing a delocalized phase in two dimensions [27] which condenses into a superconducting state. The gate voltage dependence of the diffusion coefficient previously presented corroborates this interpretation. In Fig. 3(c) we can appreciate the sharp increase of the spin-orbit coupling constant α as we move across the quantum critical point and the corresponding rise of the spin splitting Δ. This remarkable correlation between the critical temperature and the intensity of spin fluctuations is suggestive of an unconventional superconducting order parameter at the $LaAlO_3/SrTiO_3$ interface [28,29]. The large change in spin relaxation across the phase diagram, which is not yet fully understood, may result from a complex dependence of the spin-orbit coupling on band structure properties and charge profile asymmetry and should stimulate further theoretical and experimental investigations. We note that the spin splitting values can be much higher than the superconducting gap (which is of the order of 40 μeV at optimal doping) and comparable to the Fermi energy (which is of the order of 20 meV). Hence the spin-orbit coupling turns out to be an essential ingredient to describe the electronic properties of the $LaAlO_3/SrTiO_3$ interface, both in the normal and superconducting state. In conclusion, the electric field control of spin coherence at the interface between two complex oxides, $LaAlO_3$ and $SrTiO_3$, has been demonstrated. The ability to control the Zeeman and Rashba spin splitting in an oxide system is particularly promising, as fully spin polarized materials can be integrated in functional heterostructures. Moreover, this technology can be applied to nanoscale devices, where spin coherence can be manipulated by local electric fields [30].

We thank D. Jaccard, A. F. Morpurgo, M. Sigrist, and M. Bibes for useful discussions and Marco Lopes for his technical assistance. We acknowledge financial support by the Swiss National Science Foundation through the National Centre of Competence in Research ''Materials with Novel Electronic Properties'' MaNEP and Division II, by the European Union through the projects ''Nanoxide'' and ''OxIDes,'' and by the European Science Foundation through the program ''Thin Films for Novel Oxide Devices.''

[1] I. Zutic, J. Fabian, and S. D. Sarma, Rev. Mod. Phys. **76**, 323 (2004).
[2] S. Datta and B. Das, Appl. Phys. Lett. **56**, 665 (1990).
[3] Y. A. Bychkov and E. I. Rashba, J. Phys. C **17**, 6039 (1984).
[4] P. D. Dresselhaus, C. M. A. Papavassiliou, R. G. Wheeler, and R. N. Sacks, Phys. Rev. Lett. **68**, 106 (1992).
[5] J. Nitta, T. Akazaki, H. Takayanagi, and T. Enoki, Phys. Rev. Lett. **78**, 1335 (1997).
[6] J. B. Miller *et al.*, Phys. Rev. Lett. **90**, 076807 (2003).
[7] A. Ohtomo and H. Y. Hwang, Nature (London) **427**, 423 (2004).
[8] S. Thiel, G. Hammerl, A. Schmehl, C. W. Schneider, and J. Mannhart, Science **313**, 1942 (2006).
[9] A. Brinkman *et al.*, Nature Mater. **6**, 493 (2007).
[10] N. Reyren *et al.*, Science **317**, 1196 (2007).
[11] A. D. Caviglia *et al.*, Nature (London) **456**, 624 (2008).
[12] N. Reyren *et al.*, Appl. Phys. Lett. **94**, 112506 (2009).
[13] M. Basletic *et al.*, Nature Mater. **7**, 621 (2008).
[14] O. Copie *et al.*, Phys. Rev. Lett. **102**, 216804 (2009).
[15] See supplementary material at http://link.aps.org/supplemental/10.1103/PhysRevLett.104.126803 for magnetoconductance measurements in a parallel field configuration.
[16] G. Bergmann, Phys. Rep. **107**, 1 (1984).
[17] S. Hikami, A. I. Larkin, and Y. Nagaoka, Prog. Theor. Phys. **63**, 707 (1980).
[18] M. I. D'yakonov and V. I. Perel', Sov. Phys. Solid State **13**, 3023 (1972).
[19] R. J. Elliott, Phys. Rev. **96**, 266 (1954).
[20] Y. Yafet, Solid State Phys. **14**, 1 (1963).
[21] L. F. Mattheiss, Phys. Rev. B **6**, 4740 (1972).
[22] S. Maekawa and H. Fukuyama, J. Phys. Soc. Jpn. **50**, 2516 (1981).
[23] As discussed in Ref. [15], for $V > 100$ V the MF theory alone is not adequate to fit the data, indicating that additional contributions to the magnetoconductance need to be taken into account.
[24] A. Punnoose, Appl. Phys. Lett. **88**, 252113 (2006).
[25] E. L. Ivchenko, A. A. Kiselev, and M. Willander, Solid State Commun. **102**, 375 (1997).
[26] G. Salis *et al.*, Nature (London) **414**, 619 (2001).
[27] S. J. Papadakis, E. P. De Poortere, H. C. Manoharan, M. Shayegan, and R. Winkler, Science **283**, 2056 (1999).
[28] L. P. Gor'kov and E. I. Rashba, Phys. Rev. Lett. **87**, 037004 (2001).
[29] V. M. Edelstein, Phys. Rev. Lett. **75**, 2004 (1995).
[30] C. Cen, S. Thiel, J. Mannhart, and J. Levy, Science **323**, 1026 (2009).